NIH Public Access
Author Manuscript
J Funct Foods. Author manuscript; available in PMC 2010 January 1.

Published in final edited form as:
J Funct Foods. 2009 January 1; 1(1): 74–87. doi:10.1016/j.jff.2008.09.011.

Absorption, Conjugation and Efflux of the Flavonoids, Kaempferol and Galangin, Using the Intestinal CACO-2/TC7 Cell Model

Robert Barrington[1], **Gary Williamson**[2], **Richard N Bennett**[1], **Barry D Davis**[3], **Jennifer S Brodbelt**[3], and **Paul A Kroon**[1,*]

[1] Institute of Food Research, Norwich Research Park, Norwich NR4 7UA, UK

[2] Proctor Food Science Department, University of Leeds, Leeds LS2 9JT, UK

[3] Department of Chemistry and Biochemistry, The University of Texas at Austin, 1 University Station A5300, Austin TX 78712, USA

Abstract

Flavonoids are biologically active compounds in food with potential health effects. We have used the Caco-2 cell monolayer model to study the absorption and metabolism of two flavonols, a class of flavonoids, specifically kaempferol and galangin. Metabolism experiments allowed identification of 5 kaempferol conjugates: 3-, 7- and 4′-glucuronide, a sulphate and a glucurono-sulphate; and 4 galangin conjugates: 3-, 5- and 7-glucuronides, and a sulphate, using specific enzyme hydrolysis, HPLC-MS, and HPLC with post column metal complexation/tandem MS. Transport studies showed that the flavonols were conjugated inside the cells then transported across the monolayer or effluxed back to the apical side. Sulphated conjugates were preferentially effluxed back to the apical side, whereas glucuronides were mostly transported to the basolateral side. For kaempferol, a small amount of the unconjugated aglycone permeated in both directions, indicating some passive diffusion. When kaempferol-3-glucuronide and quercetin7-sulphate were applied to either side of the cells, no permeation in either direction was observed, indicating that conjugates cannot re-cross the cell monolayer. Formation of apical kaempferol-7- and 4′-glucuronides was readily saturated, whereas formation of other conjugates at the apical side and all at the basolateral side increased with increasing concentration of kaempferol, implying different transporters are responsible at the apical and basolateral sides. The results highlight the important but complex metabolic changes occurring in flavonoids during absorption.

Introduction

Flavonoids are biologically active molecules which are found in foods, and have been studied as potential components of functional foods, owing to their benefits for health (Hooper et al., 2008; Holst and Williamson, 2008). Quercetin, kaempferol and galangin are closely related flavonoids belonging to the subclass of flavonols. Quercetin and kaempferol are widespread in common foods and beverages frequently consumed by western populations such as onions, apples, red wine, tea, kale, broccoli and endive. Galangin is not so widespread in western diets, but is present in less common foods such as propolis (Quiroga et al., 2006) and in spices such as galangal (*Alpinia officinarum*; Matsuda et al., 2006), and therefore constitutes a part of

* Corresponding author: paul.kroon@bbsrc.ac.uk; Phone, +44 (0)1603 255236; FAX, +44 (0)1603 507723.

Publisher's Disclaimer: This is a PDF file of an unedited manuscript that has been accepted for publication. As a service to our customers we are providing this early version of the manuscript. The manuscript will undergo copyediting, typesetting, and review of the resulting proof before it is published in its final citable form. Please note that during the production process errors may be discovered which could affect the content, and all legal disclaimers that apply to the journal pertain.

NIH-PA Author Manuscript
NIH-PA Author Manuscript
NIH-PA Author Manuscript

NIH-PA Author Manuscript

NIH-PA Author Manuscript

NIH-PA Author Manuscript

human diets where these products are widely eaten (e.g. South America and China/Taiwan, respectively).

The metabolism of quercetin has been studied extensively in cultured cells (Kuhnle et al., 2000; Spencer et al., 1999), in rat intestine (Gee et al., 2000; Crespy et al., 2001), and in liver cells (O'Leary et al., 2003). In plants and most foods, the flavonols exist as glycosides, which on ingestion, are hydrolysed to aglycones by lactase phlorizin hydrolase, and subsequently the aglycone diffuses into the cell (Day et al., 2000; Nemeth et al., 2003). Following cellular accumulation of the aglycone, extensive metabolism occurs within the enterocytes (Petri et al., 2003). This metabolism involves the formation of a number of phase-II conjugates, most notably sulphates and glucuronides, as well as methylated and mixed conjugates. Conjugation of flavonoids has a major impact on their properties, and the resulting conjugates can be either absorbed or effluxed, by active transport. Possible transporters are MRP2 (Hu et al., 2003; Walle et al., 1999b; Walgren et al., 2000a; Walgren et al., 2000b), MRP1 (Vaidyanathan and Walle, 2003; Vaidyanathan and Walle, 2001), Pgp (Leslie et al., 2001; Zhang and Morris, 2003;), Bcrp1 (Imai et al., 2004; Sesink et al., 2005; Zhang et al., 2004;) and the OATs (Hu et al., 2003).

To date, studies concerned with flavonoid absorption have focused on transport of the aglycone (Henry et al., 2005), glycoside (Walgren et al., 2000a) or total flavonoid (Sesink et al., 2003) (Olthof et al., 2000; Murota et al., 2000), and there is a lack of knowledge concerning the individual transporters for phase II conjugates. Since flavonols are only partially bioavailable in humans, even though the portal blood facilitates removal of absorbed material to maintain a favourable concentration gradient, it would appear that metabolism affects the ability of flavonols to cross the intestinal barrier. Therefore, we have investigated the transport of two flavonols, kaempferol and galangin, using CaCo-2/TC7 cell monolayers and have paid particular attention to the formation of conjugates within the cells and their efflux from the cells.

Materials and Methods

CaCo-2/TC7 cell culture

CaCo-2/TC7 cells were a kind gift from Dr Monique Rousset (INSERM, Paris, France), and were cultured between passages 32 and 51. Cells were grown in Dulbecco Modified Eagle's Medium (DMEM) with 1% non-essential amino acids, 1% L-glutamine, 100 IU/ML penicillin and 100 μg/ml streptomycin, and supplemented with 20% (v/v) foetal calf serum. Cells were maintained in an incubator at 37°C with 5% CO_2 and 95% air. Cell seeding was assessed by light microscope and was undertaken at 80% confluency which approximated to 3 d post seeding. Cells were seeded at 2-4 × 10^4 cells per cm^2 on 10 cm dishes (growing area 75 cm^2), and allowed to grow until 21 d post confluent. Media was changed 3 times per week. Transepithelial electrical resistance of 6 and 12 well Transwells monolayers was routinely measured directly before changing cell culture media using a Millicell-ERS volt ohmmeter (Millipore Corporation, Billerica, MA, USA). Additionally TEER measurements were taken before experiments to ensure adequate monolayer integrity.

Flavonoid metabolism experiments

Prior to treatments, cells were aspirated of media and washed three times with phosphate buffered solution. Ascorbic acid (100 μmol/L) was added to foetal calf free serum and phenol red DMEM, and 10 mL of this media then added to the treatment and control dishes. Flavonols (kaempferol and galangin from Extrasynthase, Genay, France; kaempferol 3-glucuronide from IFR, Norwich, UK; quercetin 7-sulphate was a kind gift from Dr Denis Barron, Nestle Research Centre, Lausanne, Switzerland) dissolved in dimethyl sulphoxide (DMSO) (stock

NIH-PA Author Manuscript

NIH-PA Author Manuscript

NIH-PA Author Manuscript

concentrations 10 mmol/L, stored at -20°C) were added to the media, with the equivalent volume of DMSO as control. Control and treated cells were incubated at 37°C for the indicated time period. Media and cells were harvested and separately subjected to HPLC analysis both directly (non-hydrolysed) and following incubation with sulphatase and β–glucuronidase enzymes (enzyme hydrolysed), as described below.

Flavonoid transport experiments

To investigate the transport of individual flavonol conjugates, clonal CaCo-2/TC7 cell monolayers were loaded apically with 40 μmol / L of flavonol. After 60 min, samples of media were taken from the apical, basolateral and cellular compartments and analysed using HPLC for individual flavonol conjugates. The rate of individual conjugate efflux was calculated for both the apical and basolateral compartments, and these rates used to calculate an apical to basolateral ratio. This ratio is a measure of the favoured direction of efflux, with a value of over 1.0 indicating an apically favoured efflux, values below 1.0 symbolising a basolaterally favoured efflux, and values of 1.0 symbolising an equal distribution of conjugate efflux.

Analysis of media and cell samples

Cells and media were harvested and analysed by HPLC for flavonol metabolites. Glucuronidase (645,200 units per gram) and sulphatase type V from limpets (15,000 units per gram) were purchased from Sigma-Aldrich (Poole, UK). To media samples were added 0.23 mg (150 units) of glucuronidase or 10 mg (150 units) of sulphatase. Samples of the enzyme treated media (1 mL) were added to 50 μL of trifluoracetic acid (TFA) and 50 μL of acetonitrile. Samples were centrifuged at 13,000 g for 10 min before being injected onto an Agilent 1100 HPLC (Agilent, Stockport, UK) comprising of two pump units, autosampler, mixer, and a diode-array detector covering the range 200-600 nm. Portions (100 μL) of sample were injected onto a Gemini C18 narrow bore reverse-phase column (Phenomenex, Macclesfield, UK) at a rate of 0.3 mL per minute. The mobile phase consisted of acetonitrile with 0.1% TFA and MilliQ water with 0.1% TFA. Integration of peaks was performed at 370 nm and UV-visible spectra obtained. The following authentic standards were used for quantification purposes: kaempferol-3-glucuronide, which had been isolated from endive and the chemical structure verified using NMR (Dupont et al, 2000), was used for the quantification of kaempferol conjugates; kaempferol aglycone (commercial) was used to quantify kaempferol; galangin (commercial) was used to quantify galangin and the galangin metabolites.

Mass spectrometry

Electrospray ionization quadrupole ion trap mass spectrometry with collision induced dissociation (CID) (Agilent G1956B LC/MSD SL, Agilent, Stockport, UK) was used to analyze complexes in the form $[Co(II)(L\text{-}H)(Aux)]^+$ and $[Co(II)\ (L\text{-}H)\ (Aux)2]^+$, in which L is the flavonoid glucuronide or sulphate and Aux is a phenanthroline-based ligand (see Davis et al., 2006). These complexes yielded characteristic fragmentation patterns that facilitated assignment of the substitution position of the conjugates, and the methods were adapted to HPLC / tandem mass spectrometry with post-column cobalt complexation. These analyses were performed at the University of Texas and because different LC elution conditions were used (e.g. formic acid instead of TFA) the method was able to identify which glucuronide conjugates were present, but was not able to explicitly assign the conjugation position to the individual peaks.

Results

Initial HPLC analysis of media samples from CaCo-2/TC7 cells incubated with kaempferol and galangin resulted in the appearance of a number of peaks of absorbance at 270 nm that were not present in the untreated control media samples. Further, the concentration of galangin

NIH-PA Author Manuscript

NIH-PA Author Manuscript

NIH-PA Author Manuscript

and kaempferol both decreased, suggesting that the additional peaks were metabolites of the added flavonols. Separation and resolution were such that for both flavonols, all of the new peaks were sufficiently separated to allow identification of individual metabolites. Analysis of the unknown flavonol peaks was also performed using electrospray ionisation mass spectrometry in positive mode with selected ion monitoring (SIM). Further identification of putative phase-II conjugate peaks was investigated via hydrolysis of samples using glucuronidase and sulphatase enzyme preparations. In order to identify the conjugation position of galangin and kaempferol metabolites, samples were analysed using HPLC with post-column metal complexation and tandem mass spectrometry.

Identification of galangin conjugates

Media from galangin treated cells yielded several new peaks as shown in Figure 1. A peak at a 24.7 min with absorbance maxima at 270 and 370 nm corresponded with the aglycone peak in the galangin control and standard. A number of additional peaks not present in the control and standard were identified as possible galangin metabolites. Of these, only peaks at 14.6, 17.3, 18.1 and 24.1 min showed the UV spectra expected for a flavonol with two distinct peaks around 250-280 and 350-400 nm. The putative galangin metabolite peaks were labelled G1-G4.

Selected ion monitoring mass spectrometry indicated the presence of the $[M+H]^+ = 271$ ion associated with these four putative galangin metabolites, which provided strong evidence that they contained galangin. Three of the four putative metabolites (G1, G2, and G3) were also shown to contain the $[M+H]^+ = 447$ ion, suggesting the presence of a galangin monoglucuronide moiety. The remaining putative metabolite, G4, did not generate the $[M+H]^+ = 447$ ion, but did generate a $[M+H]^+ = 351$ ion, suggesting that this metabolite contained a galangin monosulphate moiety. None of the putative metabolites G1 to G4 generated detectable ion currents for galangin di-glucuronide ($[M+H]^+ = 623$), galangin disulphate ($[M+H]^+ = 431$) or galangin sulphoglucuronide ($[M+H]^+ = 527$). Enzymatic hydrolysis of media from galangin treated cell samples using glucuronidase resulted in a significant reduction in the areas of peaks G1, G2, and G3, with only a small effect on peak G4. Concomitant to the reduction for peaks G1-G3 was an increase in peak size for the parent aglycone. Addition of sulphatase to media from galangin treated cell samples decreased G4 peak size with little effect on other metabolites.

Further, post-column metal complexation-MS^2 analysis of the media samples confirmed the presence of galangin-7-glucuronide. The metal complex fragments of the remaining two glucuronides were identical. Given the structure of galangin, it is likely that one of these was the 5–glucuronide and the other the 3-glucuronide. The identity of peaks G1 and G2 were tentatively assigned as the 5- and 3-glucuronides, respectively, based on the similarity of the UV-visible spectra of G2 with that of kaempferol-3-glucuronide. The data summarising identification of galangin metabolites is shown in Table 1.

Identification of kaempferol conjugates

A number of new peaks of A_{370} from kaempferol treated media samples were identified as shown in Figure 2. A peak at a 21.9 min with absorbance maxima at 270 nm and 370 nm corresponded with the aglycone peak in the kaempferol control and standard. A number of additional peaks not present in the control and standard were identified as possible kaempferol metabolites. Of these only those running at 12.4, 12.8, 13.1, 14.0 and 18.8 min showed the UV spectra expected for a flavonoid with two distinct peaks of absorbance at around 250-280 and 350-400 nm. The UV spectral data for the putative kaempferol conjugates was compared with previous data for kaempferol metabolites using shift reagents to identify conjugation position (Day, 2000). There was a strong correlation between the spectra of the four unknown peaks

NIH-PA Author Manuscript

NIH-PA Author Manuscript

NIH-PA Author Manuscript

from these incubations and the previous reported spectral data, suggesting that the products were kaempferol-3-glucuronide (K2), kaempferol-7-glucuronide (K3), kaempferol-4′-glucuronide (K4) and unknown kaempferol-sulphate (K5). The remaining unknown flavonol peak, a suspected mixed glucuronide, was labelled K1.

Selected ion monitoring mass spectrometry indicated the presence of the $[M+H]^+ = 287$ ion associated with the five putative kaempferol metabolites (K1-K5), which strongly suggests they contain kaempferol. Four of the five putative metabolites (K1, K2, K3, and K4) were also shown to contain the $[M+H]^+ = 463$ ion, suggesting the presence of a kaempferol monoglucuride moiety. The remaining putative metabolite, K5, did not generate the $[M+H]^+ = 463$ ion, but did generate a $[M+H]^+ = 367$ ion, suggesting that this metabolite contained a kaempferol monosulphate moiety. None of the putative metabolites K1 to K5 produced ion currents for kaempferol diglucuronide ($[M+H]^+ = 639$) or kaempferol disulphate ($[M+H]^+ = 447$). Enzymatic hydrolysis of media from kaempferol treated cell samples using glucuronidase resulted in a reduction of peaks K1, K2, K3 and K4, with only a small effect on peak K5. Concomitant with this peak reduction for peaks K1-K4 was an increase in peak size for the parent aglycone. Addition of sulphatase to kaempferol containing media samples decreased K5 peak area with little effect on the other peaks. Addition of a mixture of sulphatase and glucuronidase to an isolated fraction containing peak K1 resulted in a reduction in the peak area for this metabolite to a greater extent than with administration of glucuronidase alone, in keeping with hydrolysis by both glucuronidase and sulphatase. Addition of only sulphatase enzyme resulted in a disappearance of peak K1 and an increase in the size of the aglycone peak Addition of only glucuronidase resulted in a partial decrease in peak K1 and an increase in an additional peak, which showed the same UV spectra and retention times as a previously isolated kaempferol sulphate peak (K5). Since the sulphatase used in these treatments is known to contain glucuronidase activity (source: crude ground limpets), while the glucuronidase was not contaminated with sulphatase (source: recombinant bacterial), metabolite K1 was likely to be a sulpho-glucuronide.

Samples of media containing suspected phase-II kaempferol conjugates were isolated using an HPLC fraction collector, fractions K1 to K5 were collected, and these were analysed by ^1H NMR (1D and 2D COSY) at 600MHz. Chemical shift values of ring and anomeric protons are shown in Table 2. No evidence of kaempferol conjugates was found for K1, which appeared to be a more complex mixture than the other fractions (signals consistent with a kaempferol B-ring substitution pattern were seen, but without corresponding A-ring or anomeric signals). The major component of K2 displayed a spectrum consistent with kaempferol 3-glucuronide; shift values were little changed relative to kaempferol itself, which is typical of 3-substituted flavonols. Literature data (Nawwar et al., 1984) available for this material concurred that K2 was kaempferol-3-glucuronide. The predominant component of K3 displayed a structure consistent with that expected for kaempferol 7-glucuronide; in particular the shifts of the A ring protons H-6 and H-8 were moved downfield, which is typical of 7-substituted flavonoids. The major component of K4 appeared to be kaempferol 4′-glucuronide, indicated by the typical downfield shift of H-3′ and H-5′. Finally K5 appeared to be a mixture; the two predominant components, K5A and K5B were tentatively identified as kaempferol 7-sulphate and kaempferol 3-sulphate, respectively. Negative ion mode ionization was used, and full scan spectra obtained. From this, chromatograms were constructed for each mass of interest. In addition to the peak corresponding to kaempferol aglycone, there were two peaks with the correct mass for kaempferol monoglucuronides and one for kaempferol monosulphate. Further, the metal complex of K3 generated a fragment pattern that was consistent with a 7-glucuronide substitution pattern. The metal complex fragmentation pattern of the glucuronide K2 was indicative of a 3-glucuronide substitution. The most likely identity of K2 is kaempferol-3-glucuronide, based on the UV spectra and the similar retention time to the kaempferol-3-

NIH-PA Author Manuscript

NIH-PA Author Manuscript

NIH-PA Author Manuscript

glucuronide standard. The data summarising the identification of kaempferol conjugates is shown in Table 3.

Transport of galangin

The transport of galangin across monolayers was investigated (Figure 3 and Table 4). Total conjugate production was 112 pmol/min. Apical efflux accounted for 42% (47 pmol/min) of conjugate efflux, with basolateral efflux accounting for 58% (65 pmol/min) of efflux. Cellular contents accounted for less than 0.1% of the total conjugates within the monolayer. The glucuronides showed preferential basolateral transport as demonstrated by the apical to basolateral ratio below 0.6 in all cases. Galangin-sulphate showed preferential apical transport with an apical to basolateral ratio above 13. Apical to basolateral transport of the aglycone was 0.34% of the starting amount in the apical compartment.

Transport of kaempferol

The transport of kaempferol across monolayers was also studied (Figure 4 and Table 4). Total conjugate production was 102 pmol/min. Apical transport accounted for 38% (39 pmol/min) of conjugate efflux, with basolateral efflux accounting for 62% (63 pmol/min) of efflux. Cellular contents accounted for less than 0.1% of the total conjugates within the monolayer. The glucuronides showed preferential basolateral transport as demonstrated by an apical to basolateral ratio below 0.3 in all cases. Kaempferol-sulphate showed preferential apical transport with an apical to basolateral ratio above 3.0. The sulphoglucuronide, also showed preferential basolateral transport, but to a lesser extent than the monoglucuronides. Apical to basolateral transport of the aglycone was 2.70% of the starting amount in the apical compartment.

Time dependence—The efflux of the kaempferol conjugates between 5 and 60 min was investigated with a fixed starting concentration of kaempferol (40 μM) (Figure 5, Table 5). From this data, the rate of individual conjugate efflux was calculated for both the apical and basolateral compartments, and these rates used to estimate an apical to basolateral ratio. Aglycone concentrations for apical, basolateral and cellular compartments were also measured. Generally, cellular production of phase-II conjugates was time dependent for kaempferol-sulphate, but not for kaempferol-glucuronides, and total production rates of conjugates were greater when the kaempferol aglycone was added apically rather than basolaterally. Apical loading of kaempferol aglycone resulted in time-dependent efflux of both sulphate and glucuronide conjugates. Basolateral loading of kaempferol aglycone resulted in time dependent efflux of kaempferol conjugates to the basolateral compartment, although no conjugates were detected at early time points in the apical compartment. With both apical and basolateral loading, there was an increase in the percentage of conversion of kaempferol aglycone to kaempferol conjugates with time. Apical to basolateral transport ratios were reduced with increasing concentration of aglycone when loaded apically, but we were not able to detect possible changes in apical: basolateral ratios for basolateral loading due to the low rate of conjugate production. Transport of the aglycone in apical to basolateral and basolateral to apical directions were time dependent and were similar.

Concentration dependence—CaCo-2/TC7 cells were first loaded apically or basolaterally with 5, 15, 40 or 100 μmol / L kaempferol with the opposing chamber containing media only. After 60 min, samples of media were taken from the apical, basolateral and cellular compartments and analysed using HPLC for individual kaempferol conjugates (Figure 6, Table 6). From this data, the rate of individual conjugate efflux was calculated for both the apical and basolateral compartments, and this rate used to create an apical to basolateral ratio. Aglycone concentrations for apical, basolateral and cellular compartments were also measured. Previous studies have demonstrated that some flavonols consumed in the diet may reach

NIH-PA Author Manuscript

NIH-PA Author Manuscript

NIH-PA Author Manuscript

concentrations as high as 50 μM or more in the intestinal lumen (Walgren et al., 1998). Based on this evidence a concentration range of 5 to 100 μM was considered to cover physiologically-achievable concentrations.

Generally, cellular production of phase-II conjugates was concentration-dependent and was greater when the aglycone was added apically compared to basolaterally. Cellular efflux in both an apical and basolateral direction was dependent on the concentration of kaempferol aglycone irrespective of the loading compartment, and this was seen for all the phase-II conjugates. Cellular production and cellular efflux of kaempferol-4′-glucuronide appeared to be saturated. With apical loading, increasing kaempferol aglycone concentration led to reduced percentage of conversion to conjugates. However, with basolateral loading, there was no concentration dependent effect and the conversion rate was 10-fold lower than with apical loading. Apical to basolateral transport ratios were reduced with increasing concentration of aglycone when loaded apically, but were increased when loaded basolaterally. Transport from apical to basolateral was greater than basolateral to apical.

Potential for trans-epithelial transport of conjugates and log P values—To investigate the fate of effluxed flavonol conjugates, CaCo-2/TC7 cells were grown on 12-well Transwell inserts as monolayers and isolated kaempferol 3-glucuronide or quercetin 7-sulphate was added to the apical or basolateral compartments at a concentration of 40 μM. After 60 min samples of media were taken from the apical, basolateral and cellular compartments and analysed using HPLC for individual flavonol conjugates. For kaempferol 3-glucuronide, quercetin 7-sulphate and phenol red, transport to the opposing media compartment following apical loading was 0.65, 0.69 and 1.15% of the loading amount, respectively. Following basolateral loading transport to the opposing compartment was 0.66, 1.39 and 0.77%, respectively. Transport into the cell was less than 0.001% of the loading amount for both apical and basolateral loading for all analytes. To investigate the relationship between flavonol hydrophobicity and structure, log P values were calculated and are shown in Table 7.

Discussion

Upon apical loading of flavonol aglycones to CaCo-2/TC7, either in transport or metabolism experiments, total conjugate production rate was greatest for galangin, followed by kaempferol and then quercetin (data not shown for quercetin), suggesting differing rates of phase-II conjugation and/or different rates of entry into the cells. This data is consistent with Yi et al. (2006), who showed that increasing the number of hydroxyl groups on anthocyanins decreases their absorption by CaCo-2 cells. Net transfer of kaempferol was also greater than quercetin using a perfused rat model (Crespy et al., 2003). The enzymes responsible for glucuronidation and sulphation of flavonoids in humans, UDP-glucuronysyltransferase and phenolsulphotransferase respectively, are present in CaCo-2 cells (Galijatovic et al., 2001). This occurs in vivo since kaempferol-3-glucuronide was the major metabolite in human plasma after ingestion of endive, a source of kaempferol (DuPont et al., 2004). For all flavonols, total intracellular conjugates made up less than 0.2% of the total conjugates produced at 60 min, although the actual concentrations within the cells were high (0.1 – 25 μM) due to the relatively small volume of the cells. Only a small proportion of the aglycone crosses the cells unmodified, 2.7 and 1.4% for kaempferol and galangin, respectively. For kaempferol, the transcellular aglycone rate was measured in both apical and basolateral directions. Apical to basolateral transcellular rates were more rapid than basolateral to apical transcellular rates of the unmodified aglycone, and this increased movement from the apical compartment coincided with a more rapid production of conjugates, suggesting that conjugate production is related to aglycone influx. Other authors have also noted that apical to basolateral aglycone movement exceeds that in the opposite direction (Walle et al., 1999b; Oitate et al., 2001; Ng et al., 2005). Oitate et al. (2001) suggests that this is due to a carrier-mediated system located on the

NIH-PA Author Manuscript

NIH-PA Author Manuscript

NIH-PA Author Manuscript

apical membrane, and present evidence that the apical to basolateral movement of isoflavonoids was temperature dependent, saturable and inhibited by other flavonoids. However, the possibility that an efflux transporter that recognises aglycones as a substrate and acts to increase transport of the aglycone in an apical to basolateral direction but is not present on the basolateral membrane cannot be discounted based on available data. Distinct differences exist in the efflux preference between apical and basolateral membranes for sulphate and glucuronide conjugates of kaempferol and galangin. Apical to basolateral ratios demonstrated there was a preferential efflux to the basolateral compartment for glucuronidated conjugates and preferential efflux to the apical compartment for sulphated conjugates. Mixed sulpho-glucuronides were effluxed preferentially basolaterally, and behaved in this respect like the mono-glucuronides. If glucuronides are preferentially effluxed to the basolateral compartment in CaCo-2 and CaCo-2/TC7 cells, but sulphates are preferentially effluxed to the apical compartment, it could be expected that intervention studies might reflect this by demonstrating higher levels of circulating glucuronides in the plasma. Indeed, glucuronides have been shown to be the major components of circulating flavonoids in a number of studies in both humans and animals. In a study involving analysis of rat plasma, 64% of the circulating metabolites of quercetin were glucuronide and methoxy conjugates, and 36% were sulphate conjugates (Crespy et al., 1999). The major components in plasma of humans after oral feeding of glucoside supplements were quercetin glucuronides (Sesink et al. 2001). Walle et al. (2001) detected higher levels of chrysin glucuronides than chrysin sulphates in urine of humans and the bile of rats, suggesting that these levels might reflect higher levels of circulating glucuronides.

Experiments involving the addition of glucuronides and sulphates to CaCo-2/TC7 Transwell monolayers demonstrated that effluxed conjugates are effectively trapped in the compartment they are effluxed to. In a physiological setting, this would imply that apically effluxed conjugates (predominately sulphate conjugates) remain in the gut lumen where they may be excreted in the faeces or metabolised by bacterial degradation, and that basolaterally effluxed conjugates (predominately glucuronide conjugates) enter the hepatic portal blood system and circulation. However, the uptake of conjugates depends on cell type and the nature of the conjugate. For HepG2 cells, some quercetin glucuronides were taken up and metabolised, and a proportion were even converted to sulphated conjugates. However, in fibroblasts, there was no uptake of quercetin-*O*-β-D-glucuronide (Spencer et al., 2003).

It was demonstrated for the first time in this study that kaempferol apical to basolateral transport in CaCo-2/TC7 cells was controlled by the rate of aglycone entry to the cell for some conjugates, and at the level of the cellular conjugating enzyme or the efflux transporter for other conjugates. For 3-, 7- and sulpho-glucuronide conjugates, apical to basolateral ratios did not change with increasing concentrations of kaempferol when aglycone was added to the basolateral or apical compartment, and total rates of glucuronidated conjugate transport continued to rise with increasing concentrations of kaempferol aglycone. Further, total conjugate production rates continued to increase with increasing concentrations of aglycone. This data shows that neither transporter nor enzyme saturation was evident at the concentrations of kaempferol applied (5 to 100 μM) and demonstrates that efflux is not limited at the transport or enzyme level for these conjugates. Data from time course experiments showed that maximum kaempferol concentration (around 20-25 μM) within the cell is reached within 5 min of application to the apical compartment, and this is reflected in the rates of production of 3-, 7- and sulphoglucuronide which are not time dependent. However, when loaded basolaterally, cellular levels of aglycone never exceed 2 μM and this was reflected in slow rates of production, suggesting that it is the rate of entry of aglycone to the cell that is the limiting factor and not the transport of these conjugates in CaCo-2/TC7 cells. Based on the evidence that flavonoids consumed in the diet can reach concentrations of around 50 μM in the intestinal lumen (Walgren et al., 1998), this provides further evidence that at physiological

NIH-PA Author Manuscript

NIH-PA Author Manuscript

NIH-PA Author Manuscript

levels intestinal tissue rapidly conjugates flavonols in the -3- and -7-position and provides new evidence that intestinal tissue also rapidly conjugates kaempferol to a sulpho-glucuronide conjugate. These conjugates are rapidly transported across the basolateral membrane, as reflected in studies that have shown high circulating levels of 3- and 7-glucuronidated flavonoids (Murota et al., 2000) (Moon et al., 2001) (Gee et al., 2000) (Day et al., 2001) (Dupont et al., 2004). No studies have reported on circulating levels of the sulpho-glucuronide of kaempferol, but quercetin sulpho-glucuronides have been detected in humans (Day et al., 2001).

The effect of kaempferol aglycone concentration on transport of sulphate conjugates was also determined, and it was found that increasing concentrations of kaempferol aglycone, when added apically, did cause a reduction in the apical to basolateral ratio for kaempferol sulphate. The apical to basolateral ratio of the sulphate conjugates of kaempferol consistently demonstrated values over 1 indicative of preferential apical afflux. At 100 μM kaempferol, apical transport of kaempferol sulphate became significantly reduced, however, this reduction was not concomitant with a reduction in production of kaempferol-sulphate, indicating that saturation of apical transport was occurring. With basolateral loading, rates of kaempferol-sulphate production were lower than with apical loading, and apical transport did not become saturated. This data is supported in the literature by work from Kaldas et al. (2003), who demonstrated that at low concentrations of aglycone, resveratrol-sulphate transport was preferentially apical, whereas at higher concentrations there was more of a shift towards basolateral transport. This shift may have been due to apical transporter saturation. Hu et al. (2003) also demonstrated an apical saturation of apigenin sulphate in CaCo-2 cells with high concentrations of apigenin aglycone applied to the apical compartment.

In conclusion, these data show that the flavonols kaempferol and galangin are taken up and rapidly conjugated by differentiated CaCo2 cells to yield a number of glucuronide and sulphate conjugates, most of which have been identified. These conjugates are then effluxed out of the cells to both the apical (luminal) and basolateral (serosal) sides, with glucuronides and sulphates preferentially effluxed to the basolateral and apical compartments, respectively. These observations are consistent with the predominance of glucuronidated conjugates reported previously for human plasma.

Acknowledgments

The authors thank Dr Paul Needs, Dr Russell McLauchlan and Geoff Plumb (all IFR) for providing technical assistance and advice during these studies. This research was funded by the Biotechnology and Biological Sciences Research Council (UK) through a studentship to R.B. and a Competitive Strategic Grant, and by Nestlé U.K. Ltd.

References

Crespy V, Morand C, Besson C, Cotelle N, Vezin H, Demigne C, Remesy C. The splanchic metabolism of flavonoids highly differed according to the nature of the compound. American Journal of Physiology 2003;284:980–988.

Crespy V, Morland C, Besson C, Manach C, Demigne C, Remesy C. Comparison of the intestinal absorption of quercetin, phloretin and their glucosides in rats. Journal of Nutrition 2001;131:2109–2114. [PubMed: 11481403]

Davis BD, Needs PW, Kroon PA, Brodbelt JS. Identification of isomeric flavonoid glucuronides in urine and plasma by metal complexation and LC-ESI-MS/MS. Journal of Mass Spectrometry 2006;41:911–920. [PubMed: 16810646]

Day, AJ. Uptake an metabolism of dietary flavonoid glycosides. University of East Anglia (Institute of Food Research); Norwich. UK: 2000.

Day AJ, Bao Y, Morgan MR, Williamson G. Conjugation position of quercetin glucuronides and effect on biological activity. Free Radicals in Biology and Medicine 2000;29:1234–1243.

NIH-PA Author Manuscript

NIH-PA Author Manuscript

NIH-PA Author Manuscript

Day AJ, Mellon F, Barron D, Sarrazin G, Morgan MRA, Williamson G. Human metabolism of dietary flavonoids: identification of plasma metabolites of quercetin. Free Radical Research 2001;35:941–952. [PubMed: 11811545]

Dupont MS, Day AJ, Bennett RN, Mellom FA, Kroon PA. Absorption of kaempferol from endive, a source of kaempferol-3-glucuronide in humans. European Journal of Clinical Nutrition 2004;58:947–954. [PubMed: 15164116]

Dupont MS, Mondin Z, Williamson G, Price KR. Effect of variety, processing, and storage on the flavonoid glycoside content and composition of lettuce and endive. Journal of Agriculture and Food Chemistry 2000;48:3957–3964.

Galijatovic A, Otake Y, Walle UK, Walle T. Induction of UPD-glucuronosyltransferase UGT1A1 by the flavonoid chrysin in caco-2 cells – potential role in carginogen bioactivation. Pharmaceutical Research 2001;18:374–379. [PubMed: 11442279]

Gee JM, DuPont MS, Day AJ, Plumb GW, Williamson G, Johnson IT. Intestinal transport of quercetin glycosides in rats involves both deglycosylation and interaction with hexose transport pathways. Journal of Nutrition 2000;130:2765–2771. [PubMed: 11053519]

Henry C, Vitrac X, Decendit A, Ennamany R, Krisa S, Merillon J. Cellular uptake and efflux of trans-piceid and its aglycone trans-resveratrol on the apical membrane of human intestinal Caco-2 cells. Journal of Agriculture and Food Chemistry 2005;53:798–803.

Holst B, Williamson G. Nutrients and phytochemicals: from bioavailability to bioefficacy beyond antioxidants. Current Opinion in Biotechnology 2008;19:73–82. [PubMed: 18406129]

Hooper L, Kroon PA, Rimm EB, Cohn JS, Harvey I, Le Cornu LA, Ryder JJ, Hall WL, Cassidy A. Flavonoids, flavonoid-rich foods, and cardiovascular risk: a meta-analysis of randomized controlled trials. American Journal of Clinical Nutrition 2008;88:38–50. [PubMed: 18614722]

Hu M, Chen J, Lin H. Metabolism of flavonoids via enteric recycling: mechanistic studies of disposition of apigenin in the Caco-2 cell culture model. Journal of Pharmacology and Experimental Therapies 2003;307:314–21.

Imai Y, Tsakahara S, Asada S, Sugimoto Y. Phytoestrogens/flavonoids reverse breast cancer resistance protein/ABCG2-mediated multidrug resistance. Cancer Research 2004;64:4346–4352. [PubMed: 15205350]

Kaldas MI, Walle UK, Walle T. Resveratrol transport and metabolism by human intestinal Caco-2 cells. Journal of Pharmacy and pharmacology 2003;3:307–312. [PubMed: 12724035]

Kuhnle G, Spencer JP, Schroeter H, Shenoy B, Debnam ES, Srai SK, Rice-Evans C, Hahn U. Epicatechin and catechin are *O*-methylated and glucuronidated in the small intestine. Biochemisrty and Biophysiology. Research Communication 2000;277:507–512.

Leslie EM, Mao Q, Oleschuk CJ, Deeley RG, Cole SPC. Modulation of multidrug resistance protein 1 (MRP1/ABCC1) transport and ATPase activities by interaction with dietary flavonoids. Molecular Pharmacology 2001;59:1171–1180. [PubMed: 11306701]

Matsuda H, Ando S, Kato T, Morikawa T, Yoshikawa M. Inhibitors from the rhizomes of *Alpinia officinarum* on production of nitric oxide in lipopolysaccharide-activated macrophages and the structural requirements of diarylheptanoids for the activity. Bioorganic and Medicinal Chemistry 2006;14:138–142. [PubMed: 16182539]

Min BS, Lee SY, Kim JH, Lee JK, Kim TJ, Kim DH, Kim YH, Joung H, Lee HK, Nakamura N, Miyashiro H, Hattori M. Anti-complement Activity of Constituents from the Stem-Bark of *Juglans mandshuric*. Biological and Pharmaceutical Bulletin 2003;26:1042–1044. [PubMed: 12843637]

Moon J, Tsushida T, Nakahara K, Terao J. Identification of quercetin 3-*O*-β-D-glucuronide as an antioxidative metabolite in rat plasma after oral administration of quercetin. Free Radicals in Biology and Medicine 2001;30:1274–1285.

Murota K, Shimizu S, Chujo H, Moon J, Terao J. Efficiency of absorption and metabolic conversion of quercetin and its glucuronides in human intestinal cell line Caco-2. Archives of Biochemistry and Biophysics 2000;384:391–397. [PubMed: 11368329]

Nawwar MAM, Souleman AMA, Buddrus J, Linscheid M. Flavonoids of the flowers of *Tamarix nilotica*. Phytochemistry 1984;23:2347–2349.

Nemeth K, Plumb GW, Berrin J, Juge N, Jacob R, Naim HY, Williamson G, Swallow DM, Kroon PA. Deglycosylation by small intestinal epithelial cell β-glucosidase is a critical step in the absorption

NIH-PA Author Manuscript

NIH-PA Author Manuscript

NIH-PA Author Manuscript

and metabolism of dietary flavonoid glycosides in humans. European Journal of Nutrition 2003;42:29–42. [PubMed: 12594539]

Ng SP, Wong KY, Zhang L, Zuo Z. Evaluation of the first-pass glucuronidation of selected flavones in gut by CaCo-2monolayer model. Journal of Pharmacy and Pharmaceutical Science 2005;8:1–9.

Oitate M, Nakaki R, Koyabu N, Takanaga H, Matsuo H, Ohtani H, Swada Y. Transcellular transport of genistein, a soyabean-derived isoflavone, across human colon carcinoma cell line (Caco-2). Biopharmaceutics and Drug Disposition 2001;22:23–29.

O'Leary KA, Day AJ, Needs PW, Mellon FA, O'Brien NM, Williamson G. Metabolism of quercetin-7- and quercetin-3-glucuronides by an *in vitro* hepatic model: the role of human beta-glucosidase, sulfotransferase, catechol-*O*-methyltransferase and multi-resistant protein 2 (MRP2) in flavonoid metabolism. Biochemical Pharmacology 2003;65:479–491. [PubMed: 12527341]

Olthof MR, Hollman PC, Vree TB, Katan MB. Bioavailabilities of quercetin-3-glucoside and quercetin-4′-glucoside do not differ in humans. The Journal of Nutrition 2000;130:1200–1203. [PubMed: 10801919]

Petri N, Tannergren C, Holst B, Mellon F, BAO Y, Plumb G, Bacon J, O'Leary K, Kroon P, Knutson L, Forsell P, Eriksson T, Lennernas H, Williamson G. Absorption/metabolism of sulforoph and quercetin, and regulation of phase II enzymes, in human jejunum in vivo. Drug Metabolism and Disposition 2003;31:805–813. [PubMed: 12756216]

Quiroga EN, Sampietro JR, Sgariglia MA, Vattuone MA. Propolis from the northwest of Argentina as a source of antifungal principles. Journal of Applied Microbiology 2006;101:103–110. [PubMed: 16834596]

Sesink ALA, Arts ICW, de Boer VCJ, Breedveld P, Schellens JHM, Hollman PCH, Russel FGM. Breast cancer resistance protein (BCRP1/ABCG2) limits net intestinal absorption of quercetin in rats by facilitating apical efflux of glucuronides. Molecular Pharmacology 2005;67:1999–2006. [PubMed: 15749994]

Sesink AL, O'Leary KA, Hollman PCH. Quercetin glucuronides but not glucosides are present in human plasma after consumption of quercetin-3-glucoside or quercetin-4′-glucoside. Journal of Nutrition 2001;131:1938–1941. [PubMed: 11435510]

Spencer JP, Chowrimootoo G, Choudhury R, Debnam ES, Srai SK, Rice-Evans C. The small intestine can both absorb and glucuronidate luminal flavonoids. FEBS Letters 1999;458:224–230. [PubMed: 10481070]

Spencer JPE, Kuhnle GGC, Williams RJ, Rice-Evans C. Intracellular metabolism and bioactivity of quercetin and its in vivo metabolites. Biochemistry 2003;372:173–181.

Vaidyanathan JB, Walle T. Transport and metabolism of the tea flavonoid (-)-epicatechin by the human intestinal cell line Caco-2. Pharmaceutical Research 2001;18:1420–1425. [PubMed: 11697467]

Vaidyanathan JB, Walle T. Cellular uptake and efflux of the tea flavonoid (-) epicatechin-3-gallate in the human intestinal cell line Caco-2. Journal of Pharmacology and Experimental Therapies 2003;307:745–52.

Walgren RA, Karnaky KJ, Lindenmayer GE, Walle T. Efflux o dietary flavonoid quercetin-4′-β-glucoside across human intestinal Caco-2 cell monolayers by apical multidrug resistance-associated protein-2. The Journal of Pharmacology and Experimental Therapeutics 2000a;294:830–836. [PubMed: 10945830]

Walgren RA, Lin J, Kinne RK, Walle T. Cellular uptake of dietary flavonoid quercetin-4′-β-glucoside by sodium-dependent SGLT1. The Journal of Pharmacology and Experimental Therapeutics 2000b; 29:4. 837–843.

Walgren RA, Walle UK, Walle T. Transport of quercetin and its glucosides across human epithelial Caco-2 cells. Biochemical Pharmacology 1998;55:1721–1727. [PubMed: 9634009]

Walle T, Otake Y, Brubaker JA, Walle UK, Halushka PV. Disposition and metabolism of the flavonoid chrysin in normal volunteers. Journal of Clinical Pharmacology 2001;51:143–146.

Walle UK, Galijatovic A, Walle T. Transport of the flavonoid chrysin and its conjugated metabolites by the human intestinal cell line Caco-2. Biochemical Pharmacology 1999b;58:431–438. [PubMed: 10424761]

NIH-PA Author Manuscript

NIH-PA Author Manuscript

NIH-PA Author Manuscript

Zhang S, Morris ME. Effects of flavonoids biochanin A, morin, phloretin, and silymarin on P-glycoprotein-mediated transport. The Journal of Pharmaceutical and Experimental Therapeutics 2003;304:1258–1267.

Zhang Z, Yang X, Morris ME. Flavonoids are inhibitors of breast cancer resistance protein (ABCG2)-mediated transport. Molecular Pharmacology 2004;65:1208–1216. [PubMed: 15102949]

NIH-PA Author Manuscript

NIH-PA Author Manuscript

NIH-PA Author Manuscript

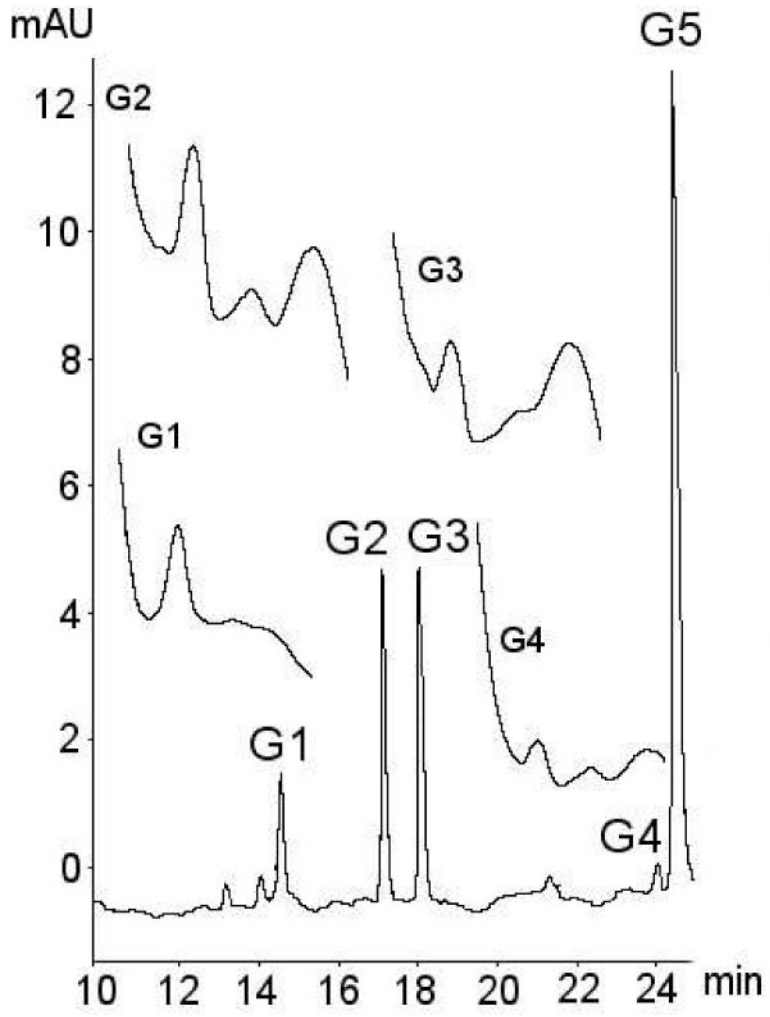

Figure 1. Identification of galangin metabolites from CaCo-2/TC7 cells and associated media

Typical chromatogram showing metabolites of galangin. The identities of metabolites was confirmed using a combination of retention time, selected ion monitoring LC/MS, tandem mass spectrometry with metal complexation, enzyme hydrolysis with sulphatase and glucuronidase, and UV spectra. No pure authentic standards were available for galangin metabolites. Suspected metabolites are labelled G1-G4, with galangin aglycone (identified by use of an authentic standard) labelled G5.

NIH-PA Author Manuscript
NIH-PA Author Manuscript
NIH-PA Author Manuscript

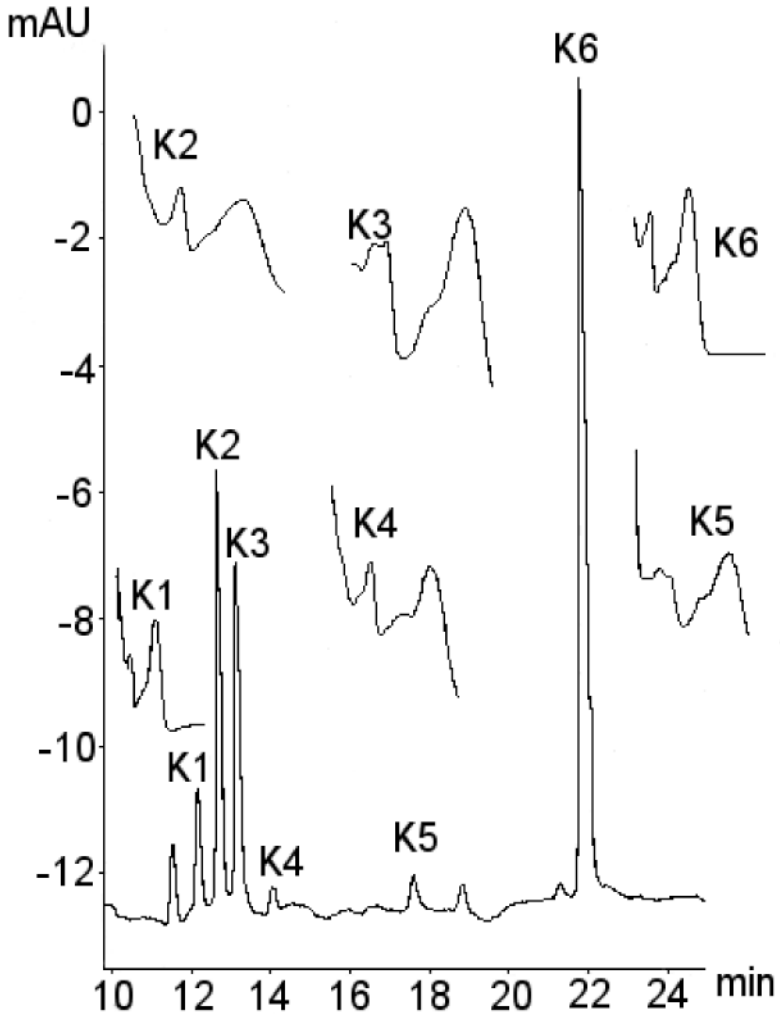

Figure 2. Identification of kaempferol metabolites from CaCo-2/TC7 cells and associated media

Typical chromatogram showing metabolites of kaempferol. The identities of metabolites were confirmed using a combination of retention time, selected ion monitoring LC/MS, tandem mass spec with metal complexation, kaempferol-3-glucuronide pure authentic standard, enzyme hydrolysis with sulphatase and glucuronidase and UV spectra. Suspected metabolites labelled K1-K5, with kaempferol aglycone labelled K6. UV spectra for the various metabolite peaks also shown with UV peak absorbance at around 250-280 nm and 350-400 nm.

NIH-PA Author Manuscript
NIH-PA Author Manuscript
NIH-PA Author Manuscript

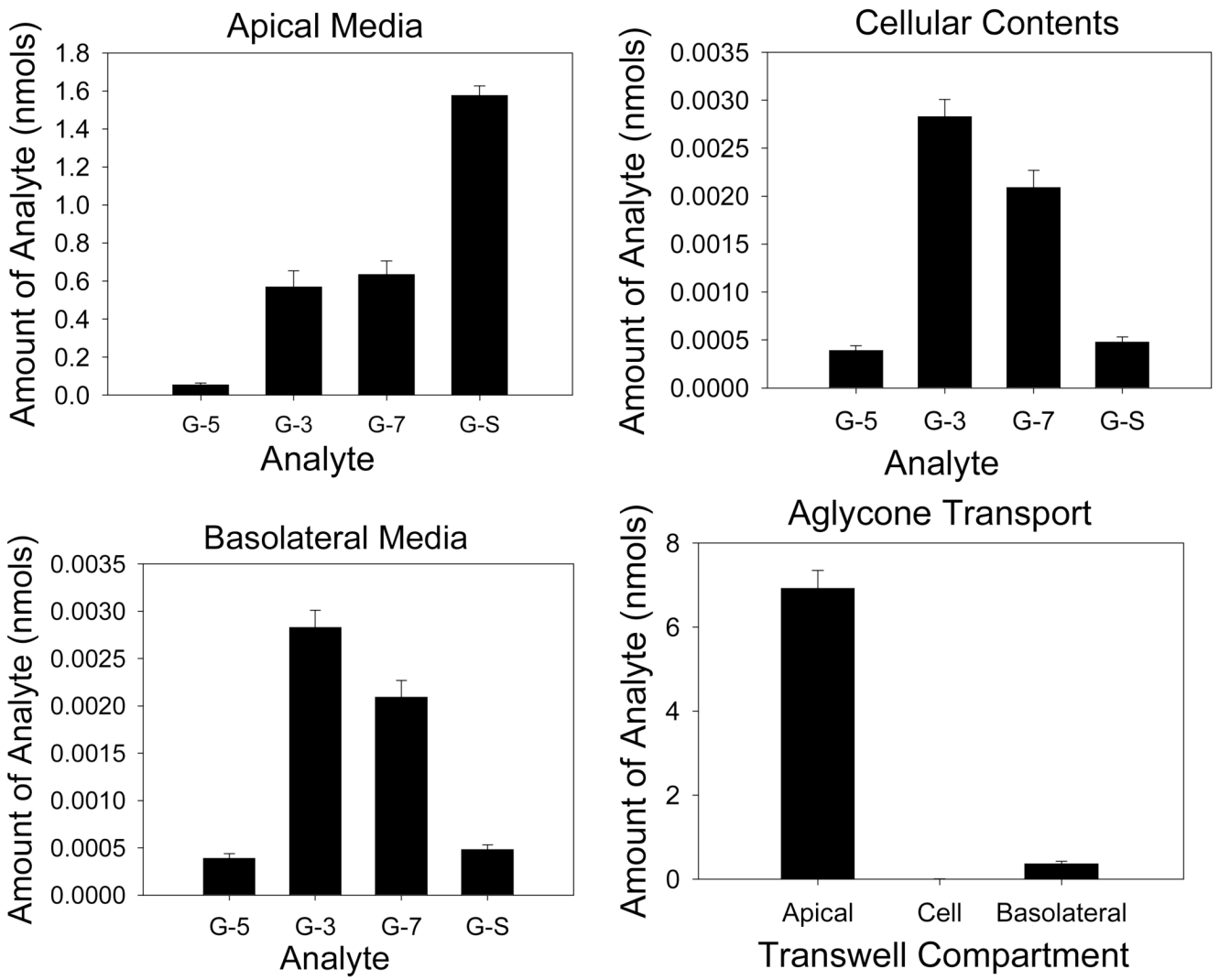

Figure 3. Transport of individual galangin conjugates in CaCo-2/TC7 cell monolayers

Graphs are presented for galangin conjugate transport in apical, cellular and basolateral compartments with apical loading of the galangin (40 μM), as well as for the transport of galangin aglycone. N=6 for all data. G-5 = galangin-5-glucuronide, G-3 = galangin-3-glucuronide, G-7 = galangin-7-glucuronide, G-S = galangin sulphate.

NIH-PA Author Manuscript

NIH-PA Author Manuscript

NIH-PA Author Manuscript

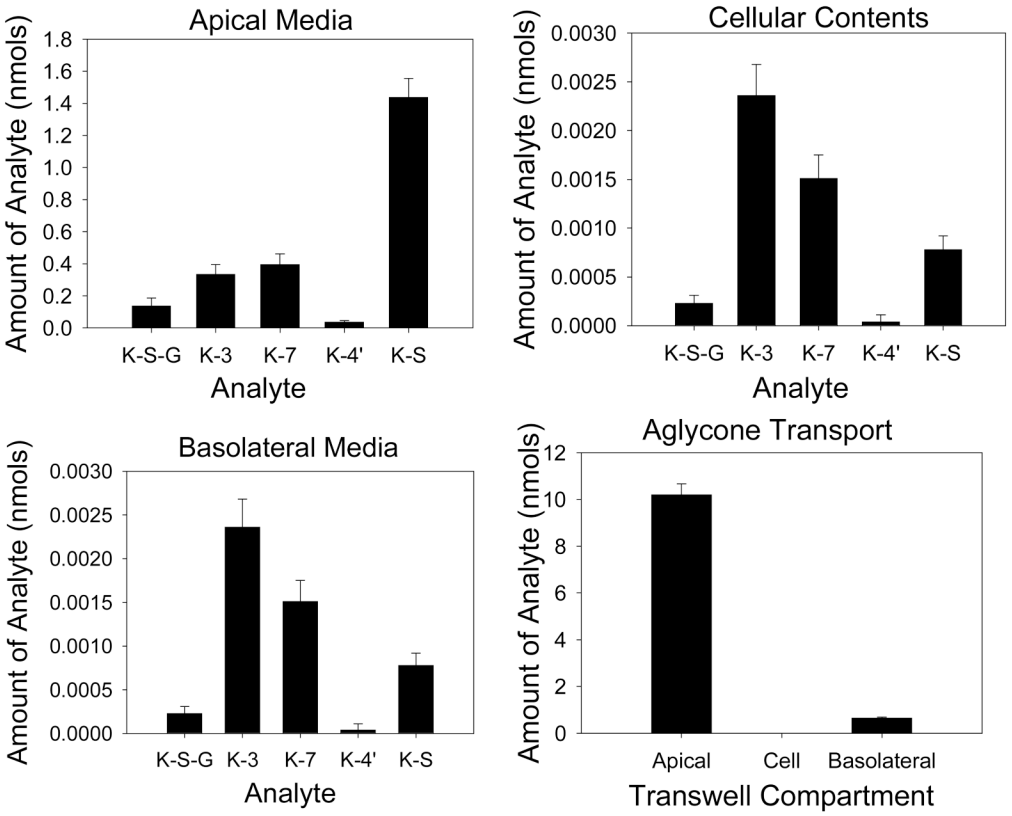

Figure 4. Transport of individual kaempferol conjugates in CaCo-2/TC7 cell monolayers

Graphs are presented for kaempferol conjugate transport in apical, cellular and basolateral compartments with apical loading of the kaempferol (40 μM), as well as for the transport of kaempferol aglycone. N=4 for all data. K-S-G = kaempferol-sulpho-glucuronide, K-3 = kaempferol-3-glucuronide, K-7 = kaempferol-7-glucuronide, K-4′ = kaempferol-4′-glucuronide, K-S = kaempferol sulphate.

NIH-PA Author Manuscript
NIH-PA Author Manuscript
NIH-PA Author Manuscript

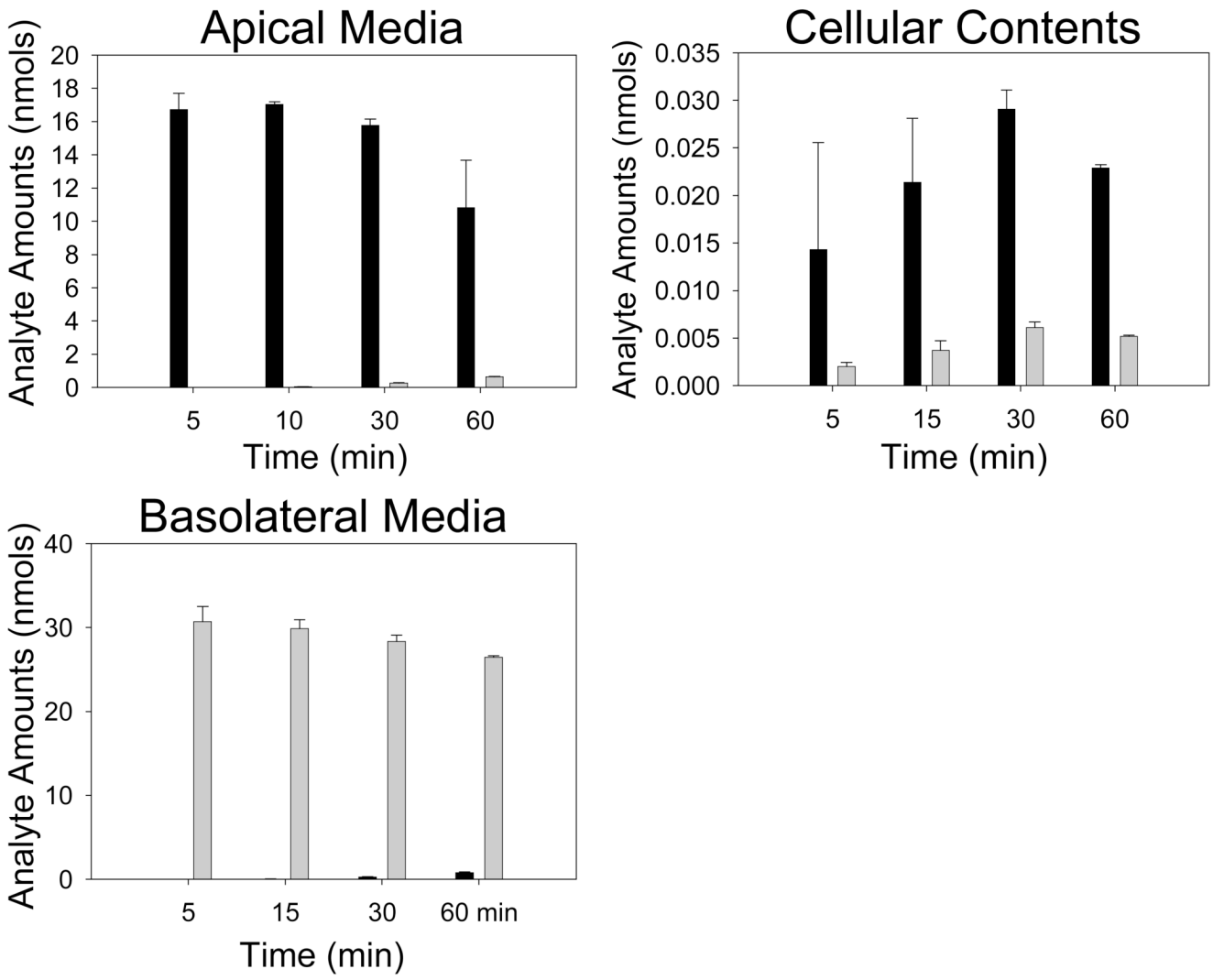

Figure 5. Aglycone transport in CaCo-2/TC7 monolayers at varying time points

Graphs are presented for the aglycone transport in apical, cellular and basolateral compartments with apical and basolateral loading of the kaempferol (40 μM, various time points). Dark bars = apical loading, light bars = basolateral loading. N = 3 for all data. All values as nmols of analyte.

NIH-PA Author Manuscript
NIH-PA Author Manuscript
NIH-PA Author Manuscript

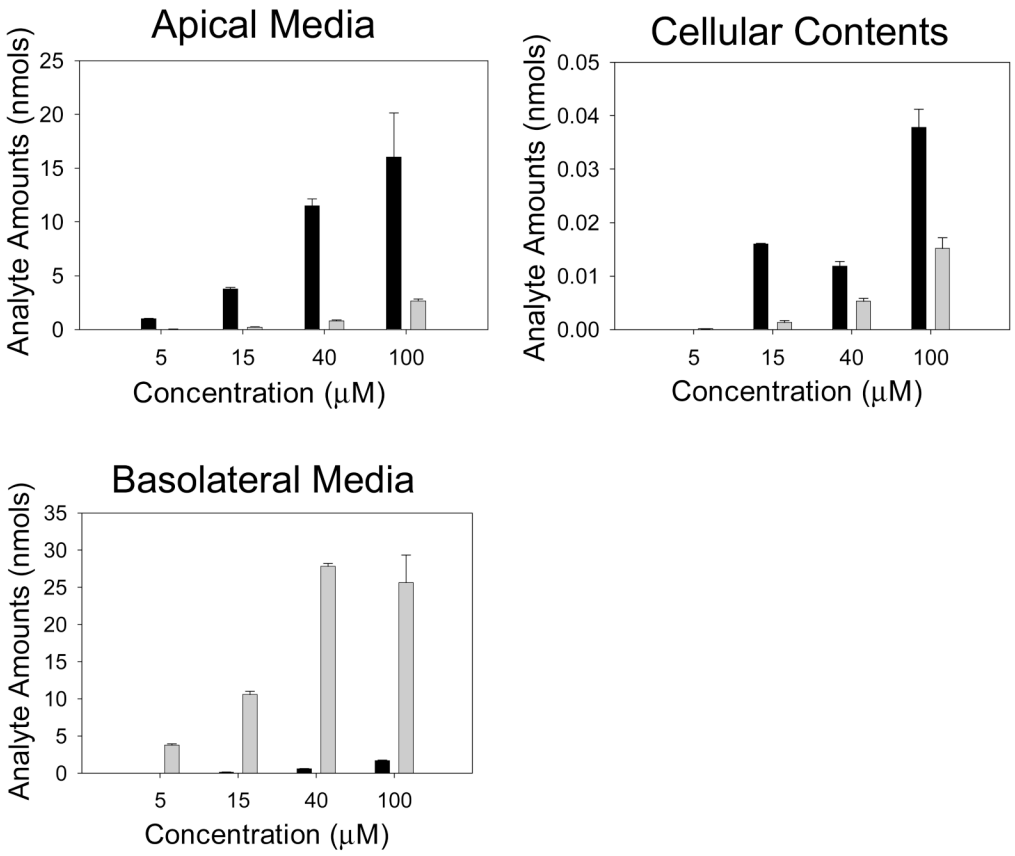

Figure 6. Aglycone transport in CaCo-2/TC7 monolayers with varying concentrations of kaempferol

Graphs are presented for kaempferol aglycone transport in apical, cellular and basolateral compartments with apical and basolateral loading of the kaempferol (60 min, various concentrations). Dark bars = apical loading, light bars = basolateral loading. N = 3 for all data. All values as nmols of analyte.

NIH-PA Author Manuscript NIH-PA Author Manuscript NIH-PA Author Manuscript

Table 1

Summary of the data used to identify galangin phase-II conjugates produced by CaCo-2/TC7 cells.

Galangin conjugate[a]	$[M+H]^+ = 463$ detected?	$[M+H]^+ = 376$ detected?	UV Trace	Standard	Treatment with glucuronidase	Treatment with sulphatase	Probable identification
G1	Yes	No	Flavonol-like[b].	None available	Rapid disappearance of peak with increase in aglycone	Minimal effect	G-5-GlcA
G2	Yes	No	Flavonol-like[b]. Spectrum similar to K-3-GlcA (K2); see Table 3 and Figure 3.	None available	Rapid disappearance of peak with increase in aglycone	Minimal effect	G-3-GlcA
G3	Yes	No	Flavonol-like[b]. Spectrum similar to K-7-GlcA (K3); see Table 3 and Figure b3.	None available	Rapid disappearance of peak with increase in aglycone	Minimal effect	G-7-GlcA
G4	No	Yes	Flavonol-like[b].	None available	Very minimal peak disappearance over hours that might be due to oxidation	Rapid disappearance of peak	G-S (unknown conjugation position)

[a] Refer to figure 1 for the corresponding chromatogram.

[b] Distinct bands at 250-280 nm and 350-400 nm.

NIH-PA Author Manuscript
NIH-PA Author Manuscript
NIH-PA Author Manuscript

Table 2

^{1}H NMR shifts/δ (DMSO-d6) for putative kaempferol metabolites.

Proton Position	K[a]	K2 (K3GlcA?)	K3GlcA[b]	K3 (K7GlcA?)	K4 (K4′GlcA?)	K5A (K7S?)	K5B (K3S?)
H-2′, H-6′	8.03	8.02	8.00	8.06	8.13	8.06	8.00
H-3′, H-5′	6.92	6.87	6.88	6.93	7.19	6.93	6.91
H-8	6.40	6.43	6.40	6.82	6.46	6.97	6.42
H-6	6.16	6.21	6.20	6.43	6.19	6.54	6.19
H-1″	-	5.48	5.40	5.26	5.18	-	-

[a] Min et al (2003)

[b] Nawwar et al (1984)

[c] Distinct bands at 250-280 nm and 350-400 nm.

NIH-PA Author Manuscript
NIH-PA Author Manuscript
NIH-PA Author Manuscript

Table 3

Summary table showing the identification of kaempferol phase-II conjugates produced in CaCo-2/TC7 cells.

Kaempferol conjugate[a]	$[M+H]^+$ = 463 detected	$[M+H]^+$ = 376 detected	UV Trace	Standard	Hydrolysis with β-glucuronidase	Hydrolysis with aryl-sulphatase	NMR	Probable identification
K1	Yes	Yes	Flavonol-like[b]	None available	Rapid disappearance of peak with increase in K-S	Minimal effect	Inconclusive	K-S-GlcA
K2	Yes	No	Flavonol-like[b]. Spectrum similar to K-3-GlcA previously identified using shift reagents[a]	Peak RT similar to K-3-GlcA standard	Rapid disappearance of peak with increase in aglycone	Minimal effect	Suggests K-3-GlcA	K-3-GlcA
K3	Yes	No	Flavonol-like[b]. Spectrum similar to K-7-GlcA previously identified using shift reagents[a]	None available	Rapid disappearance of peak with increase in aglycone	Minimal effect	Suggests K-7-GlcA	K-7-GlcA
K4	Yes	No	Flavonol-like[b]. Spectra similar to K-4′-GlcA previously identified using shift reagents[a]	None available	Rapid disappearance of peak with increase in aglycone	Minimal effect	Suggests K-4′-GlcA	K-4′GlcA
K5	No	No	Flavonol-like[b].	None available	Very minimal peak disappearance over hours that might be due to oxidation	Rapid disappearance of peak	Suggest mixture of K-3-S and K-7-S	K-S (likely to be a mixture of 3- and 7-

[a] Refer to figure 2 for the corresponding chromatogram.

[b] Distinct bands at 250-280 nm and 350-400 nm.

[c] Day (2000).

NIH-PA Author Manuscript

NIH-PA Author Manuscript

NIH-PA Author Manuscript

Table 4

Transport of individual flavonol conjugates in CaCo-2/TC7 cell monolayers to the apical and basolateral media.

Conjugate	Apical Transport (pmol / min) (average ± SD)	Basolateral Transport (pmol / min) (average ± SD)	Ap:Ba Ratio
G-5-GlcA	0.91 (± 0.15)	4.75 (± 0.57)	0.19
G-3-GlcA	9.49 (± 1.41)	38.9 (± 3.10)	0.24
G-7-GlcA	10.6 (± 1.18)	19.6 (± 1.56)	0.54
G-S	26.3 (± 0.83)	1.94 (± 0.20)	13.5
K-S-GlcA	2.46 (± 0.90)	3.90 (± 0.26)	0.59
K-3-GlcA	5.68 (± 1.21)	25.8 (± 1.79)	0.22
K-7-GlcA	6.76 (± 1.27)	23.6 (± 1.47)	0.28
K-4′-GlcA	0.65 (± 0.16)	2.27 (± 0.16)	0.26
K-S	23.3 (± 1.80)	7.69 (± 0.99)	3.02

The rate of efflux of galangin and kaempferol conjugates to the apical and basolateral compartments during 60 min incubation was measured, and values expressed as the apical to basolateral transport ratio. A value of less that 1.0 indicates preferential basolateral transport. A value of greater than 1.0 indicates preferential apical transport; n=6 for all galangin conjugates; n=4 for kaempferol conjugates, parentheses indicate standard deviation.

NIH-PA Author Manuscript
NIH-PA Author Manuscript
NIH-PA Author Manuscript

J Funct Foods. Author manuscript; available in PMC 2010 January 1.

Table 5

Total kaempferol conjugation production and apical to basolateral ratios in clonal CaCo-2/TC7 cell monolayers at varying time points.

		K-S-GlcA	K-3-GlcA	K-7-GlcA	K-4′-GlcA	K-S	Total Conjugates	Total Aglycone	% Conjugate Conversion
Apical Loading	5 min	0.00 (N/D)	0.26 (N/D)	0.00 (N/D)	0.00 (N/D)	0.00 (N/D)	0.26	16.7	2
	10 min	0.00 (N/D)	0.27 (12.7)	0.03 (N/D)	0.00 (N/D)	0.00 (N/D)	0.30	17.1	2
	30 min	0.07 (0.32)	0.47 (1.73)	0.19 (0.24)	0.00 (N/D)	0.04 (N/D)	0.77	16.1	5
	60 min	0.19 (0.29)	0.77 (0.38)	0.52 (0.24)	0.06 (N/D)	0.26 (1.53)	1.80	11.6	13
Basolateral Loading	5 min	0.00 (N/D)	0.00 (N/D)	0.00 (N/D)	0.00 (N/D)	0.00 (N/D)	0.00	30.7	0
	10 min	0.00 (N/D)	0.00 (N/D)	0.00 (N/D)	0.00 (N/D)	0.00 (N/D)	0.00	29.9	0
	30 min	0.03 (N/D)	0.07 (N/D)	0.15 (0.24)	0.03 (N/D)	0.00 (N/D)	0.28	28.6	1
	60 min	0.09 (0.47)	0.29 (0.15)	0.61 (0.41)	0.16 (0.38)	0.25 (1.47)	1.39	27.1	5

Values shown are nmols of analyte. Percentage conjugate conversion represents the total percentage of conjugation from parent aglycone. The percentage of conversion to phase-II conjugates increased in time in both the apical and basolateral compartments. The apical to basolateral ratio (numbers in parentheses) represents the apical transport rate divided by the basolateral transport rate. A value of <1.0 indicates preferential basolateral transport, while a value of >1.0 indicates preferential apical transport. Kaempferol loading concentration was 40 mM; n=3 for all data; N/D indicates not determined (usually because conjugates were not detected in one of more compartments).

NIH-PA Author Manuscript NIH-PA Author Manuscript NIH-PA Author Manuscript

Table 6

Total kaempferol conjugation production and apical to basolateral ratios in clonal CaCo-2/TC7 cell monolayers with varying concentrations of kaempferol.

		K-S-GlcA	K-3-GlcA	K-7-GlcA	K-4′-GlcA	K-S	Total Conjugates	Total Aglycone	Conjugate Conversion (%)
Apical Loading	5 μM	0.02 (N/D)	0.16 (0.22)	0.78 (0.74)	0.26 (0.44)	0.26 (N/D)	1.48	0.99	60
	15 μM	0.12 (0.47)	0.61 (0.14)	1.32 (0.23)	0.19 (0.20)	1.01 (3.46)	3.24	3.88	46
	40 μM	0.33 (0.37)	1.44 (0.15)	1.34 (0.21)	0.10 (N/D)	1.36 (2.26)	4.57	12.1	27
	100 μM	0.62 (0.28)	2.27 (0.20)	1.76 (0.20)	0.07 (N/D)	1.11 (2.04)	5.83	17.7	25
Basolateral Loading	5 μM	0.00 (N/D)	0.02 (N/D)	0.19 (2.09)	0.06 (1.56)	0.01 (N/D)	0.28	3.82	7
	15 μM	0.03 (0.56)	0.08 (0.17)	0.27 (0.72)	0.08 (0.57)	0.06 (0.83)	0.52	10.8	5
	40 μM	0.06 (.058)	0.21 (0.20)	0.34 (0.50)	0.07 (0.59)	0.17 (0.85)	0.85	28.6	3
	100 μM	0.17 (0.58)	0.67 (0.26)	0.45 (0.61)	0.05 (0.96)	0.28 (1.28)	1.62	28.3	5

Values shown are nmols of analyte. Percentage conjugate conversion represents the total percentage of conjugation from parent aglycone. The percentage of conversion to phase-II conjugates decreased with increasing concentration of kaempferol aglycone in the apical compartment. However, this concentration dependent effect of conjugate conversion was not seen with basolateral loading. Apical to basolateral ratio (numbers in parentheses) represents the apical transport rate divided by the basolateral transport rate A value of <1.0 indicates preferential basolateral transport, a value of >1.0 indicates preferential apical transport; n=3 for all data; time = 60 min.

NIH-PA Author Manuscript

NIH-PA Author Manuscript

NIH-PA Author Manuscript

Table 7

Log P values for various flavonols and flavonol conjugates.

Flavonol	Log *P* Value	Previously reported values
Quercetin	1.683	1.82[a] (Rothwell et al, 2005) 1.15[b] (Yang et al, 2001a) 1.2[a] (Brown et al, 1998) 2.15[a] (Crespy et al, 2003) 2.239[b] (Crespy et al, 2003) 2.6[a] (Vaidynathan and Walle, 2002) 2.74[b] (Sergediene et al, 1999) 0.35[b] (Murata et al, 2004)
Quercetin-4′-GlcA	-0.455	
Quercetin-3-GlcA	-0.486	
Quercetin-7-GlcA	-0.227	
Quercetin-5-GlcA	-0.486	
Quercetin-3′-GlcA	-0.455	
Quercetin-Rutinoside	n/d	0.37[a] (Brown et al, 1998)
Kaempferol	2.172	3.11[a] (Rothwell et al, 2005) 1.69[b] (Yang et al, 2001a) 69.5[a] (Brown et al, 1998) 2.94[a] (Crespy et al, 2003) 2.441[b] (Crespy et al, 2003) 0.74[b] (Murata et al, 2004) 2.69[b] (Sergediene et al, 1999)
Kaempferol-5-GlcA	0.0030	
Kaempferol-7-GlcA	0.263	
Kaempferol-4′-GlcA	0.263	
Kaempferol-3-GlcA	0.0030	
Galangin	2.651	1.25[b] (Yang et al, 2001a)
Galangin-5-GlcA	0.482	
Galangin-7-GlcA	0.742	
Galangin-3-GlcA	0.482	

[a] Experimentally determined Log P values.

[b] values obtained using computer-generated algorithms.